SUPPLEMENTARY APPENDIX

D' domain region Arg782-Cys799 of von Willebrand factor contributes to factor VIII binding

Małgorzata A. Przeradzka,[1] Josse van Galen,[1] Eduard H.T.M. Ebberink,[1] Arie J. Hoogendijk,[1] Carmen van der Zwaan,[1] Koen Mertens,[1] Maartje van den Biggelaar[1] and Alexander B. Meijer[1,2]

[1]Department of Molecular and Cellular Hemostasis, Sanquin Research, Amsterdam and [2]Department of Biomolecular Mass Spectrometry and Proteomics, Utrecht Institute for Pharmaceutical Sciences, Utrecht University, Utrecht, the Netherlands

 doi:10.3324/haematol.2019.221994

Received: March 20, 2019.

Accepted: September 25, 2019.

Pre-published: September 26, 2019.

Correspondence: *ALEXANDER B. MEUJER* - s.meijer@sanquin.nl

Supplements

Supplementary methods:

Hydrogen- Deuterium Exchange Mass Spectrometry

4.5 µM D'-D3 was pre-incubated in presence or absence of FVIII in 1:1 molar ratio for 5 min at 4˚C in binding buffer (20 mM HEPES, 150 mM NaCl and 10 mM $CaCl_2$). Samples were subsequently placed in a LEAP PAL pipetting robot (LEAP Technologies, Morrisville, NC, USA). Samples were diluted 10 times in deuterated binding buffer (98% D_2O) (Sigma-Aldrich, St Louis, USA) or standard binding buffer and incubated for 10 sec, 100 sec or 1000 sec at 24 ˚C. Deuterium exchange was quenched by mixing the sample 1:1 with quenching solution (1 g TCEP dissolved in 2 ml 2M Urea, 1M NaOH) for 5 min at 4 ˚C. The sample was digested by passing it over a Poroszyme Immobilized Pepsin Cartridge (Thermo Scientific) with an isocratic flow of 5% acetonitrile, 0.1% formic acid for 5 minutes at 4 ˚C. After collection on a trap (Acclaim Guard Column. 120, C18, 5 µm, 2.0x10 mm Thermofisher), the peptides were washed for 30 sec at 4 ˚C. Subsequently, peptides were eluted and passed over an analytic C18 column (Hypersil Gold C18, Thermo) using a gradient from 4-64% acetonitrile at 50 µl/min at 4 ˚C. Peptides were injected online into an LTQ Orbitrap-XL (Thermo Scientific) operating in positive mode. In order to identify peptides and their retention times, peptides were fragmented by collision induced dissociation. The resulting data was analysed using PEAKS software (PEAKS 7.0, Bioinformatics Solutions Inc.). Deuterium uptake of the samples was calculated using HDExaminer 2.2.0 (Sierra Analytics). Three independent experiments were performed to collect to the required data. In the figures, data are presented as percent of deuterium update calculated respectively to peptide size and maximal amount of deuterium incorporation. The results were visualised on a 3D model using PyMol (Schrödinger, Cambridge, MA, USA).

Immunosorbent assay

The anti-VWF monoclonal antibody CLB-RAg20 (2.5 µg/ml) was immobilized overnight at 4˚C in a buffer containing 50 mM $NaHCO_3$ pH 9.8 in a 96-wells microtiter plate (Nunc Maxisorp). The plate was washed 3 times with 50 mM Tris (pH 7.4), 150 mM NaCl, 5 mM $CaCl_2$, 0.1% Tween 20. Then VWF and VWF-Glu787Gln (0.25 nM) were added in a buffer containing 50 mM Tris pH 7.4, 150 mM NaCl, 5 mM $CaCl_2$, 1% bovine serum albumin, 0.1% Tween-20 to anti-VWF antibody coated plate and incubated for 2h at 37 ˚C. The unbound VWF was washed with 50 mM Tris (pH 7.4), 150 mM NaCl, 5 mM $CaCl_2$, 0.1% Tween 20. Next, increasing concentrations of FVIII (0,01875-1,2 nM) were added to the plate and incubated for 45 min at 37 ˚C. The bound FVIII was detected with an HRP-labelled monoclonal antibody (CAg 12)[1] after another 45 min of incubation 37 ˚C.

Bibliography

1. Meems H, Van Den Biggelaar M, Rondaij M, et al. C1 domain residues Lys 2092 and Phe 2093 are of major importance for the endocytic uptake of coagulation factor VIII. *Int. J. Biochem. Cell Biol.* 2011;43(8):1114–1121.

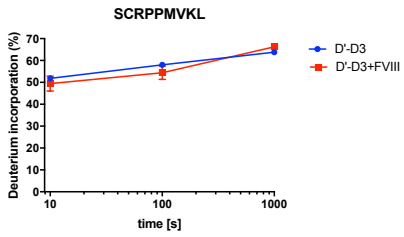
SCRPPMVKL
D'-D3
D'-D3+FVIII
Deuterium incorporation (%)
time [s]

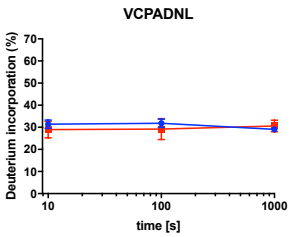
VCPADNL
Deuterium incorporation (%)
time [s]

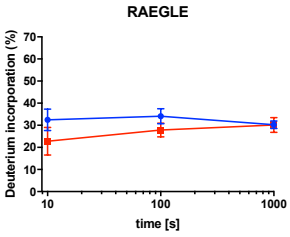
RAEGLE
Deuterium incorporation (%)
time [s]

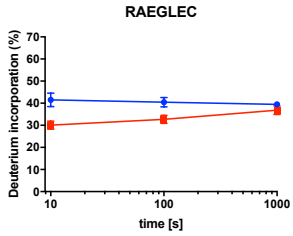
RAEGLEC
Deuterium incorporation (%)
time [s]

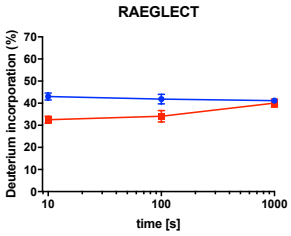
RAEGLECT
Deuterium incorporation (%)
time [s]

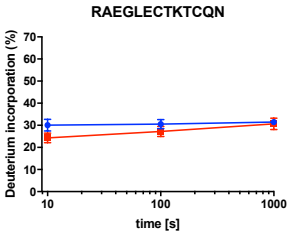
RAEGLECTKTCQN
Deuterium incorporation (%)
time [s]

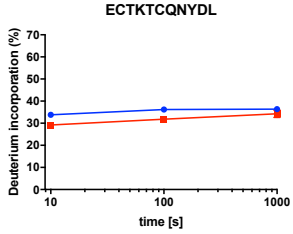
ECTKTCQNYDL
Deuterium incorporation (%)
time [s]

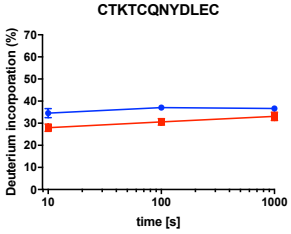
CTKTCQNYDLEC
Deuterium incorporation (%)
time [s]

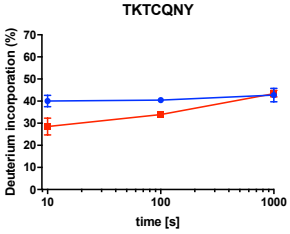
TKTCQNY
Deuterium incorporation (%)
time [s]

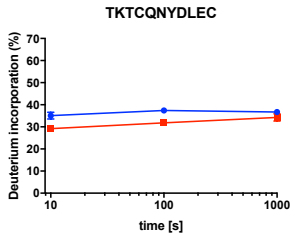
TKTCQNYDLEC
Deuterium incorporation (%)
time [s]

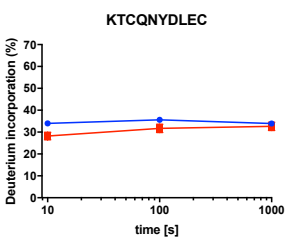
KTCQNYDLEC
Deuterium incorporation (%)
time [s]

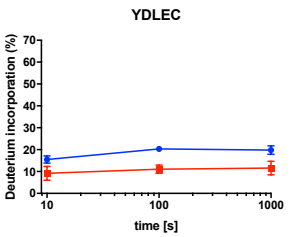
YDLEC
Deuterium incorporation (%)
time [s]

GCVSGCLCPPGMVRHENRC

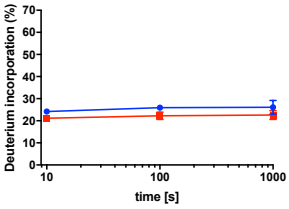

GCVSGCLCPPGMVRHENRCVA

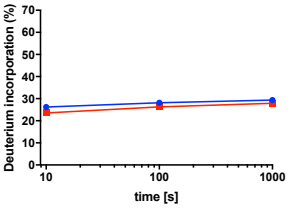

HQGKEYAPGET

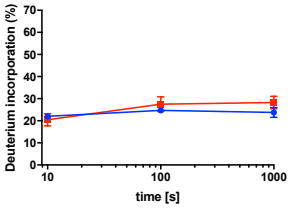

HQGKEYAPGETVKIGCN

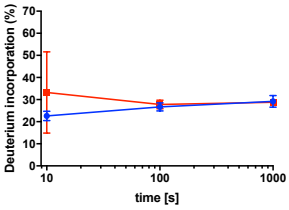

HQGKEYAPGETVKIGCNT

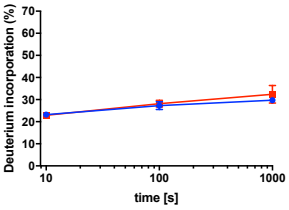

STIGMAHY

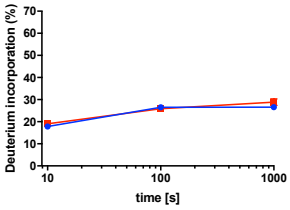

STIGMAHYLTF

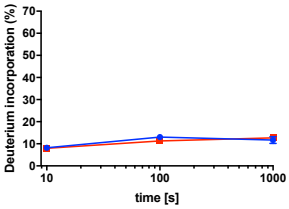

STIGMAHYLTFDGL

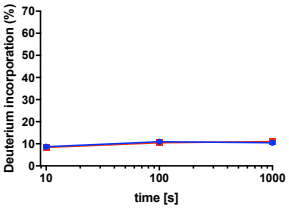

STIGMAHYLTFDGLKYLFPGECQ

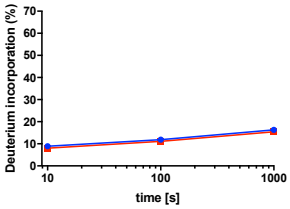

STIGMAHYLTFDGLKYLFPGECQY

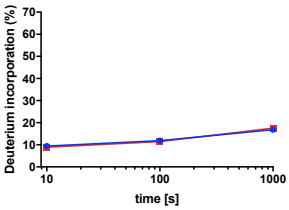

IGMAHY

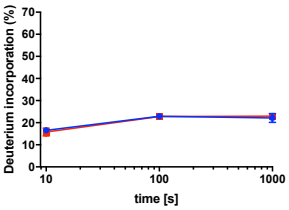

IGMAHYLTF

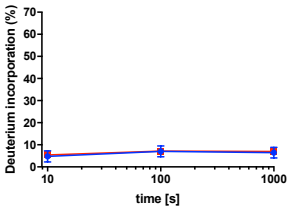

IGMAHYLTFDGL

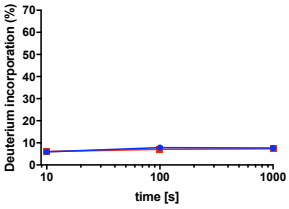

IGMAHYLTFDGLKYLFPGE

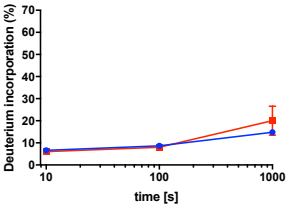

IGMAHYLTFDGLKYLFPGECQ

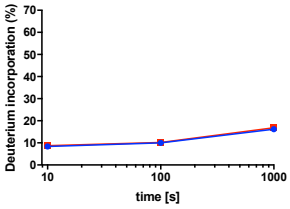

MAHYLTF

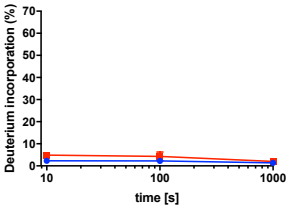

AHYLTFDGLKYLFPGECQY

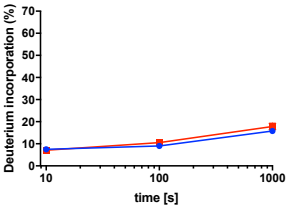

LTFDGL

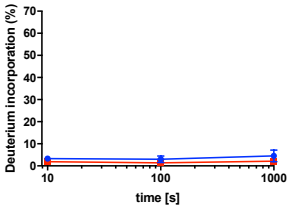

LTFDGLKYLFPGECQ

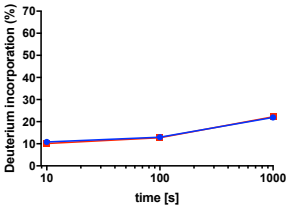

LTFDGLKYLFPGECQY

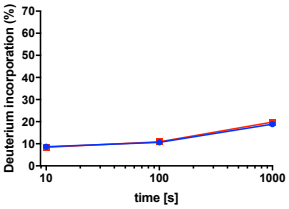

DGLKYLFPGE

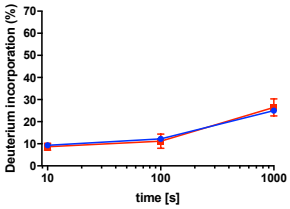

DGLKYLFPGEC

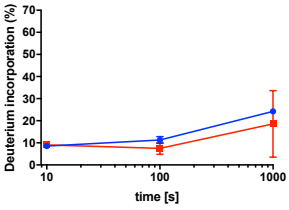

DGLKYLFPGECQ

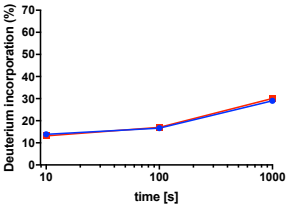

DGLKYLFPGECQY

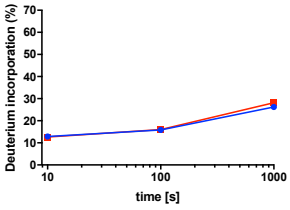

DGLKYLFPGECQYVL

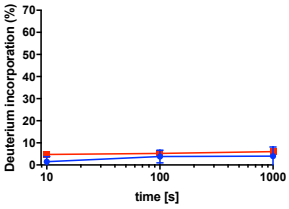

KYLFPGEC

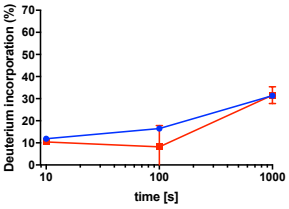

KYLFPGECQ

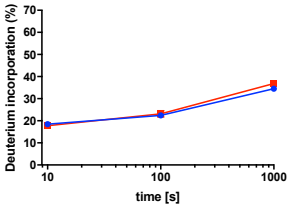

KYLFPGECQY

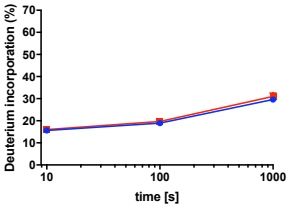

VLVQDYCGSNPGT

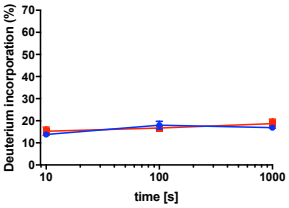

VLVQDYCGSNPGTF

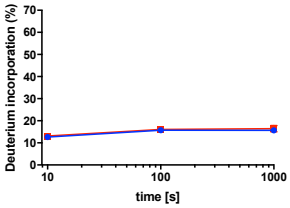

VQDYCGSNPGTF

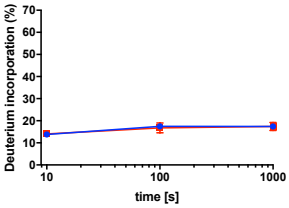

YCGSNPGTF

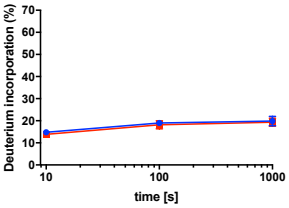

FRILVGNKGCSHPSVKCKKRVTIL

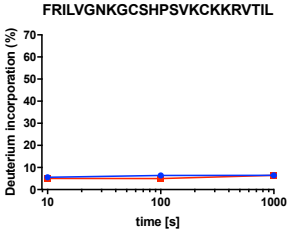

RILVGNKGCSHPSVKCKKRVTIL

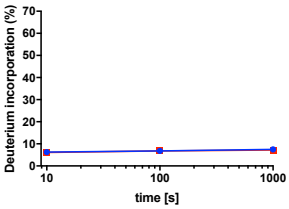

VEGGEIEL

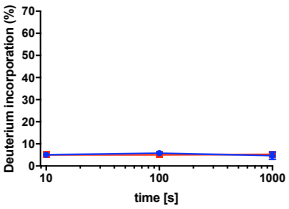

IELFDGEVNVKRPMKDETHF

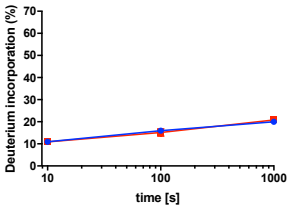

LFDGEVNVKRPMKDETHF

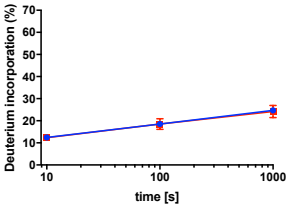

FDGEVNVKRPMKDETHF

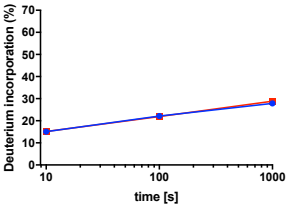

EVNVKRPMKDETHF

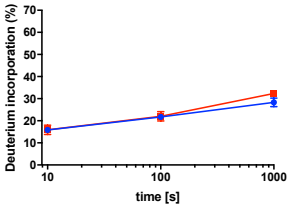

VNVKRPMKDETHF

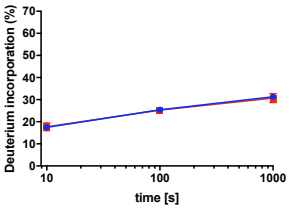

VKRPMKDETHF

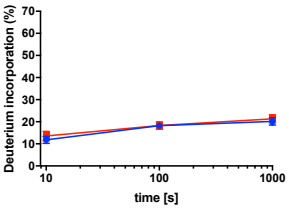

EVVESGRY

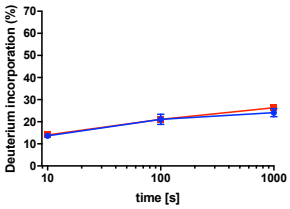

IILLLGKALSV

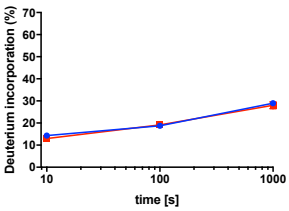

IILLLGKALSVVWDRHLSISV

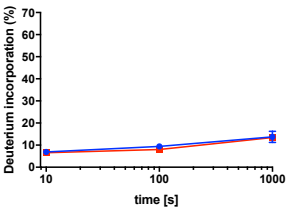

IILLLGKALSVVWDRHLSIS

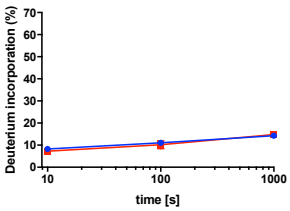

LLGKALSV

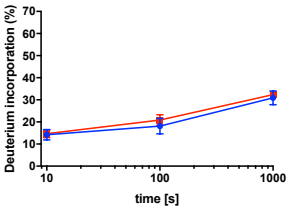

LLGKALSVVW

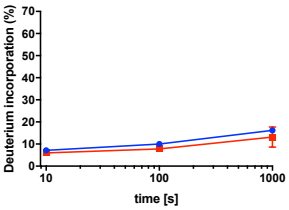

LLGKALSVVWDRHLSIS

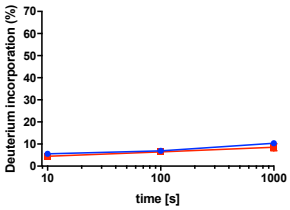

LGKALSV

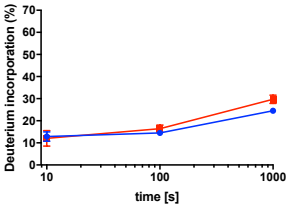

LGKALSVVW

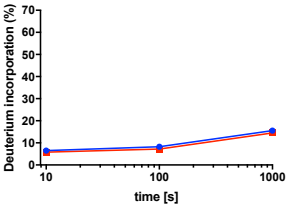

LGKALSVVWDRHLSIS

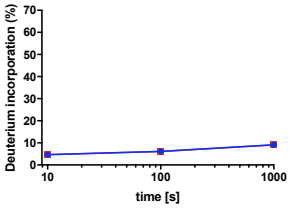

LGKALSVVWDRHLSISV

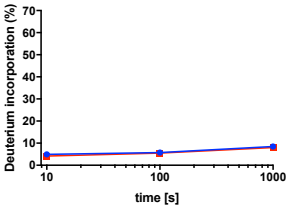

LSVVWDRHLSISV

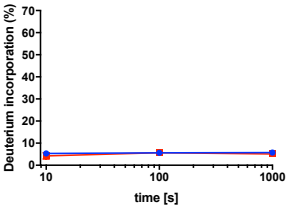

VVWDRHLSIS

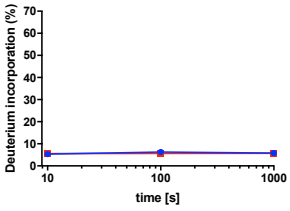

VVWDRHLSISV

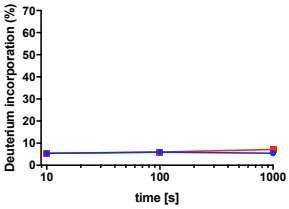

VWDRHLSI

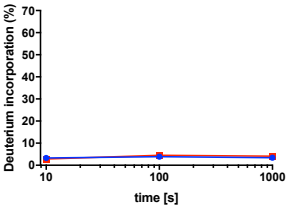

VWDRHLSIS

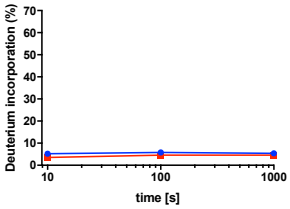

VVLKQTYQE

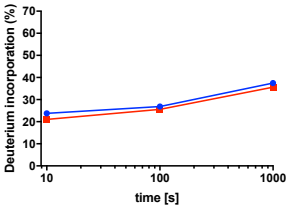

VVLKQTYQEKVCG

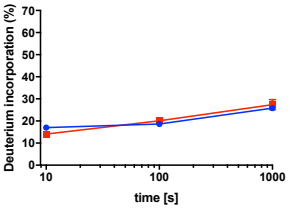

VVLKQTYQEKVCGL

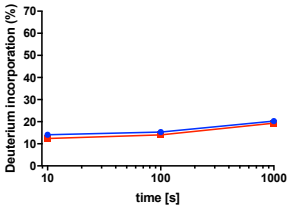

VLKQTYQE

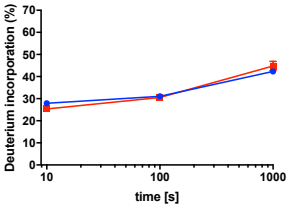

VLKQTYQEKVCG

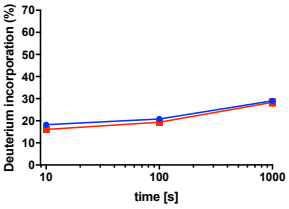

VLKQTYQEKVCGL

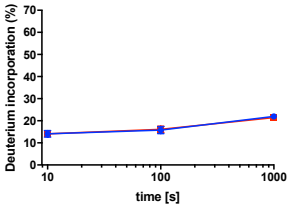

LKQTYQEKVCGL

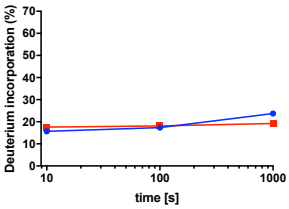

KQTYQEKVCGL

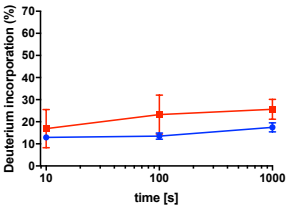

KQTYQEKVCGLCGNF

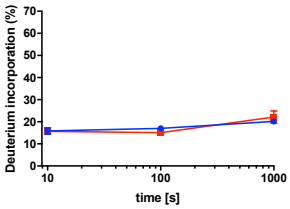

KVCGLCGNF

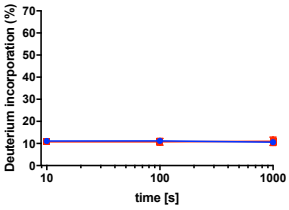

CGNFDGIQNNDLTSSNL

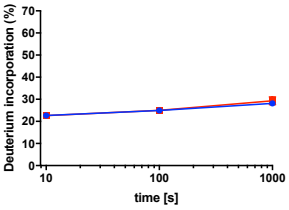

DGIQNNDLTSSNL

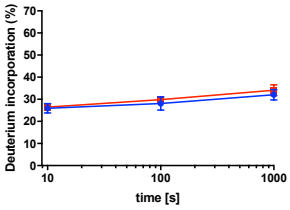

QVEEDPVDFGNS

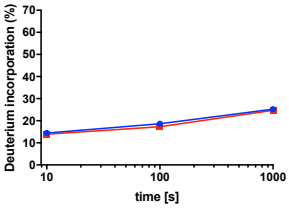

QVEEDPVDFGNSW

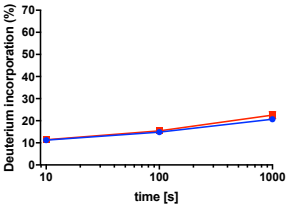

PVDFGNS

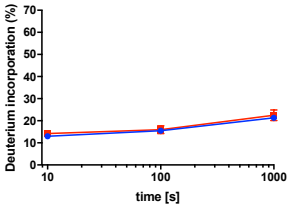

PVDFGNSW

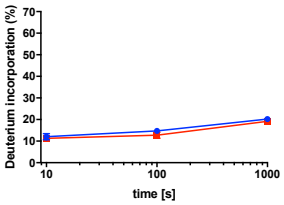

WKVSSQ

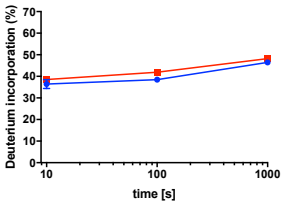

WKVSSQC

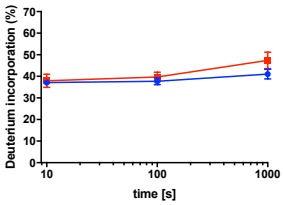

WKVSSQCAD

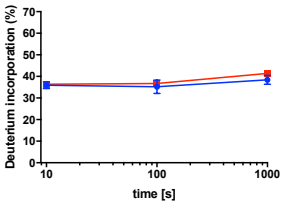

WKVSSQCADTRKVPLDSSPATCHN

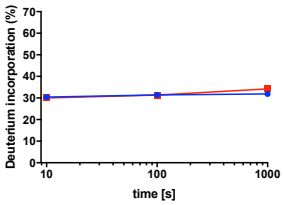

WKVSSQCADTRKVPLDSSPATCHNNIM

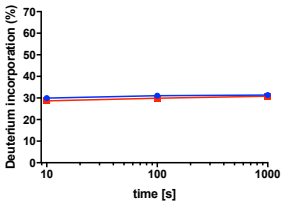

WKVSSQCADTRKVPLDSSPATCHNNIMKQTMVDSSC

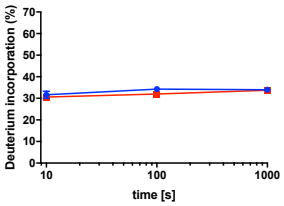

CADTRKVPLDSSPATCHN

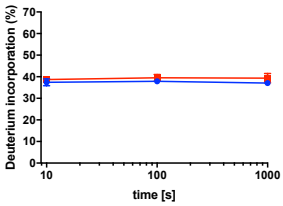

CADTRKVPLDSSPATCHNNIM

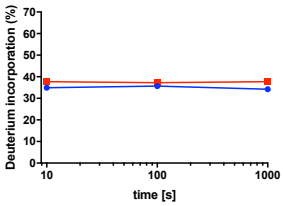

ADTRKVPLDSSPATCHN

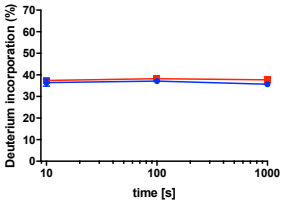

ADTRKVPLDSSPATCHNNIM

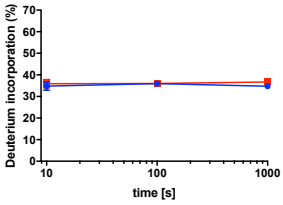

DTRKVPLDSSPATCHN

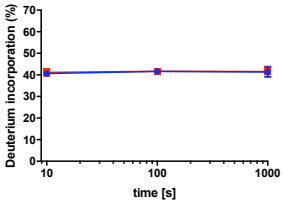

DTRKVPLDSSPATCHNNIM

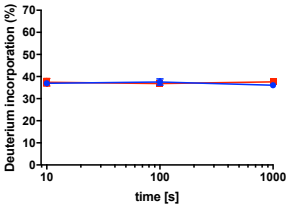

TRKVPLDSSPATCHN

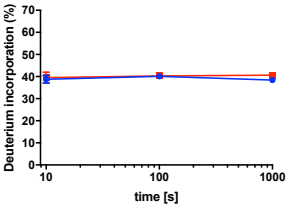

RKVPLDSSPATCHN

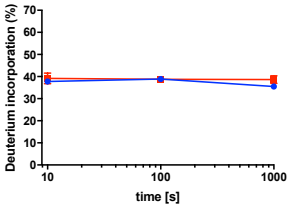

RKVPLDSSPATCHNNIM

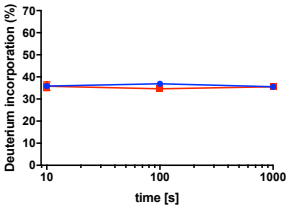

RILTSDV

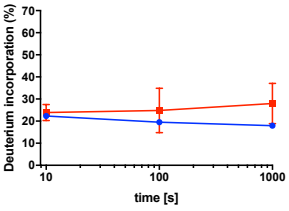

FQDCNKLVDPEPYL

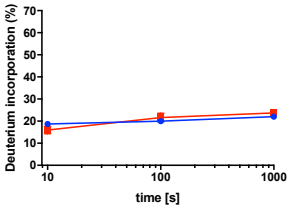

FQDCNKLVDPEPYLDV

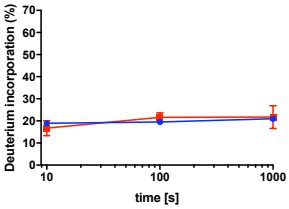

YAHVCAQHGKVVT

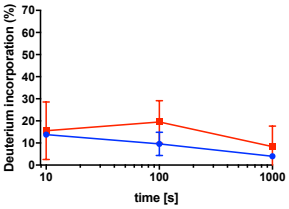

YAHVCAQHGKVVTWRTATLCPQSC

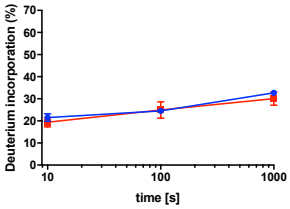

EERNLRENGYESE

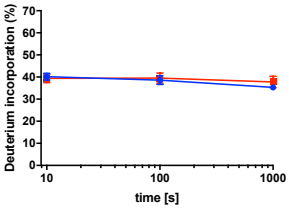

RNLRENGYESE

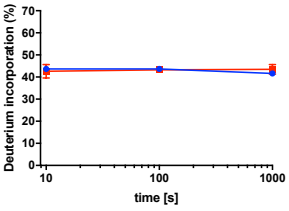

LRENGYESE

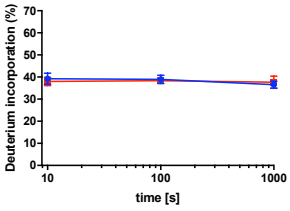

WRYNSCAPAC

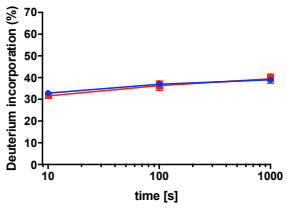

WRYNSCAPACQ

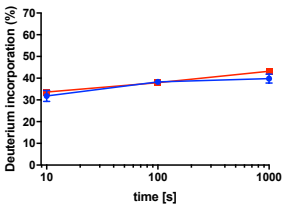

WRYNSCAPACQV

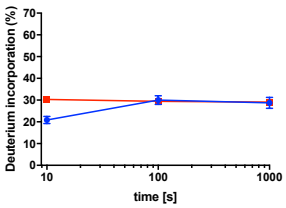

QVTCQHPEPLAC

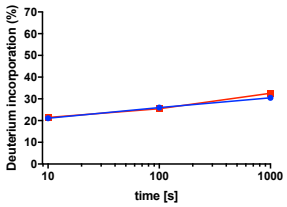

VTCQHPEPLAC

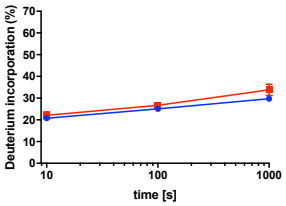

VTCQHPEPLACPVQ

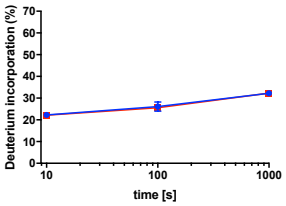

PVQCVEGCHAHCPPGKILDEL

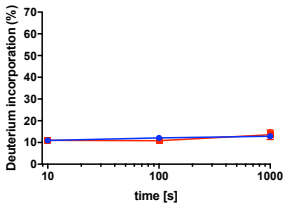

PVQCVEGCHAHCPPGKILDELLQTCVDPEDCPVCE

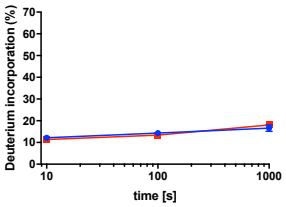

CVEGCHAHCPPGKILDEL

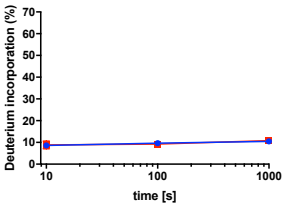

CVEGCHAHCPPGKILDELLQTCVDPEDCPVCE

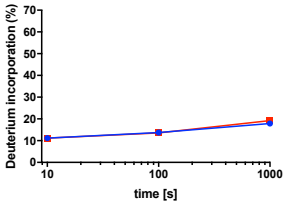

VEGCHAHCPPGKILDEL

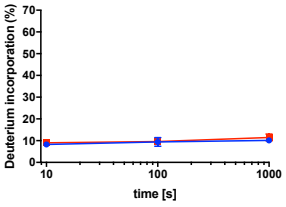

VEGCHAHCPPGKILDELLQTCVDPEDCPVCE

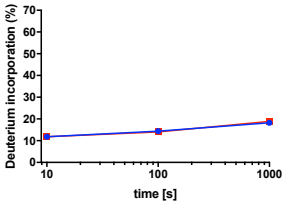

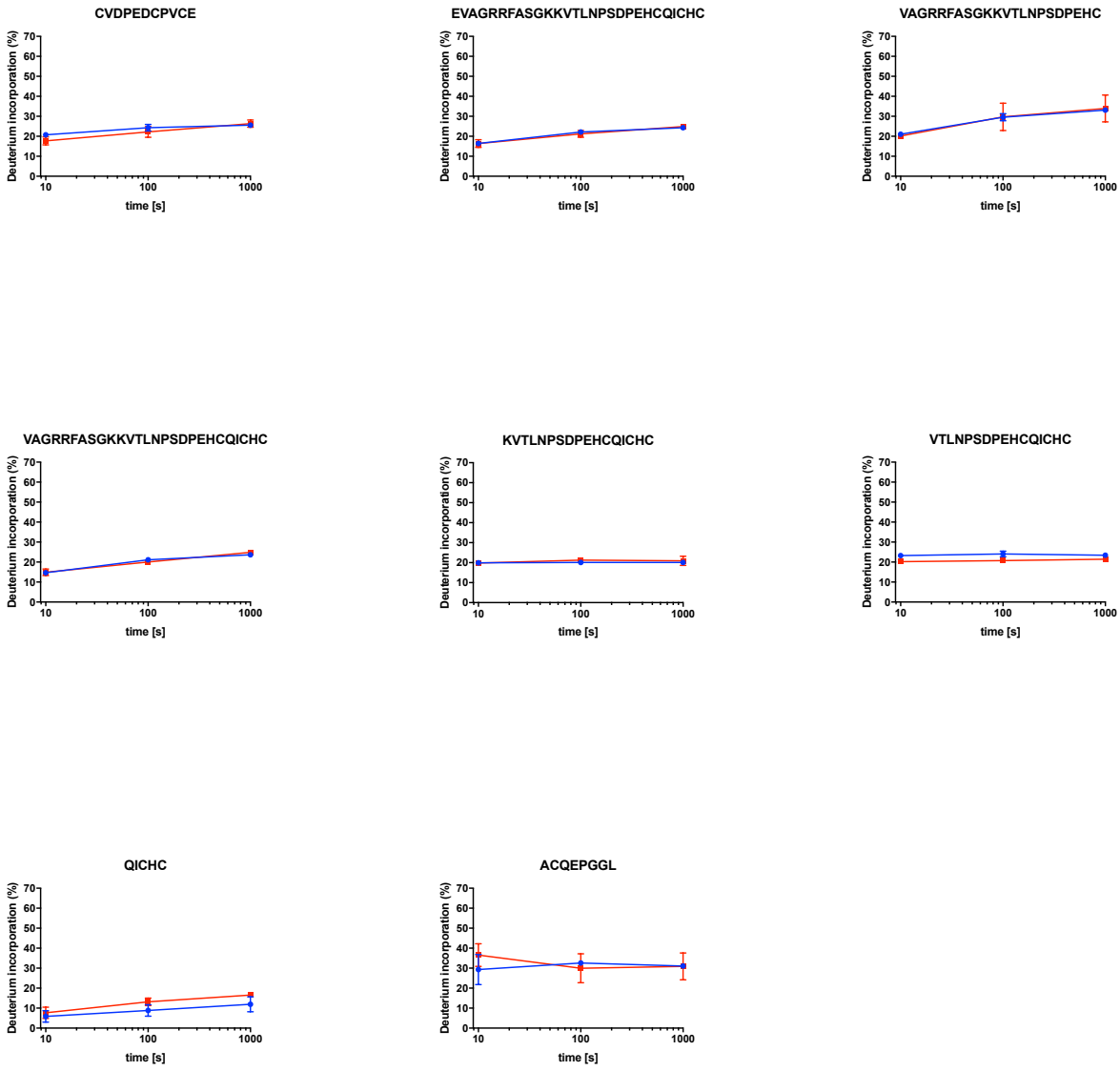

Supplemental Figure S1. HDX-MS analysis of D'-D3 in presence and absence of FVIII. D'-D3 was incubated for 10s, 100s and 1000s in a deuterium buffer consisting of 20 mM HEPES (pH 7.4), 150 mM NaCl and 5 mM $CaCl_2$ in presence or absence of FVIII. The proteins were processed for HDX-MS analysis as described in methods. Shown is the percentage of deuterium incorporation of the indicated peptides as a function of time. Data represents mean ± SD of three independent experiments.

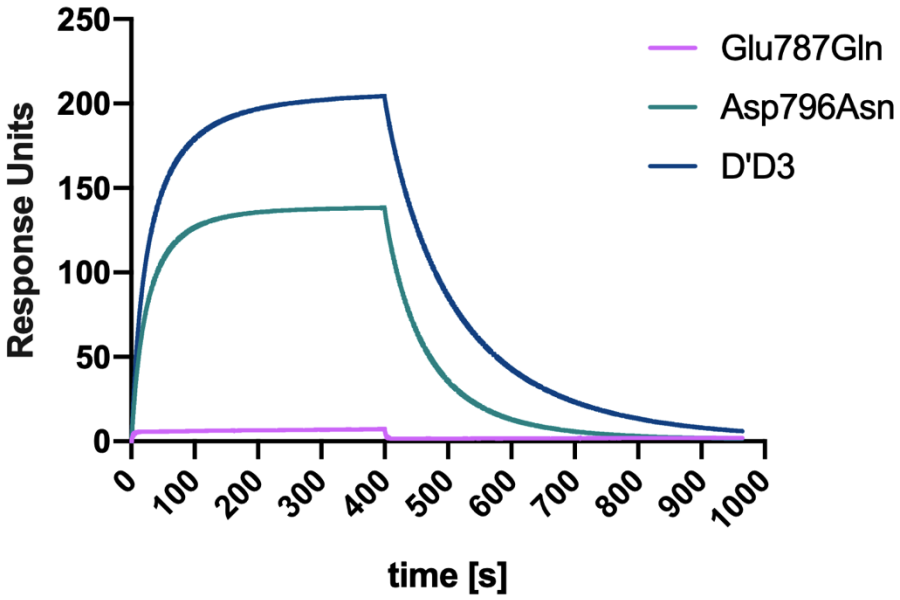

Supplemental Figure S2. SPR analysis of D'D3 variants Glu787Gln and Asp796Asn in interaction with FVIII. 200 nM of the D'-D3 variants were passed over FVIII that was immobilized via antibody EL14 to the surface of a CM5 sensor chip as described in the methods section of the manuscript. The binding response is represented in Response Units and was assessed in 20 mM HEPES (pH 7.4), 150 mM NaCl, 5 mM $CaCl_2$, 0.05% (v/v) Tween 20 at a flow rate of 30 µl/min at 25ºC.

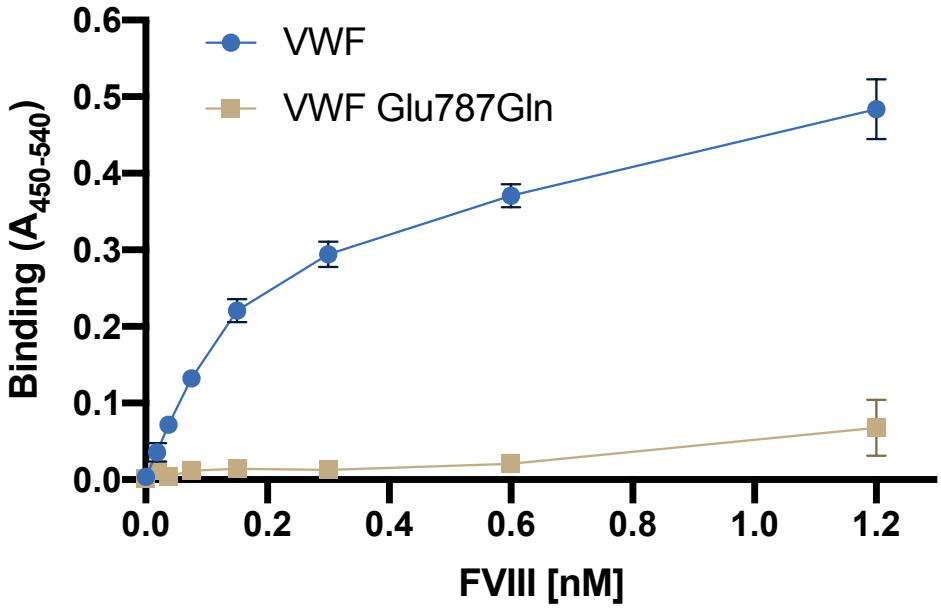

Supplemental Figure S3. Changing Glu787 for Gln in full length VWF affects FVIII binding
Increasing concentrations of FVIII were added to WT-VWF or VWF Glu787Gln that was immobilized via antibody Rag-20 in a buffer comprising of 50 mM Tris pH 7.4, 150 mM NaCl, 5 mM $CaCl_2$, 1% bovine serum albumin, 0.1% Tween-20. FVIII binding to immobilized VWF was assessed employing HRP-conjugated CAg12. The binding curves were corrected for the binding response that was measured in the absence of VWF. Data represents mean ± SD of three independent experiments.

Supplemental Figure S4. Crystal structure of D'-D3 in a ribbon representative in yellow. Residues Arg782-Cys799 and Lys773 are shown in blue represented by sticks. The C1 domain of FVIII is shown in a ribbon presentation in green.

peptide number	sequence	domain
1	SCRPPMVKL	TIL'
2	SCRPPMVKLVCPADNL	
3	VCPADNL	
4	NLRAEGLEC	
5	RAEGLE	
6	RAEGLEC	
7	RAEGLECT	
8	RAEGLECTKTCQN	
9	RAEGLECTKTCQNYDLEC	
10	ECTKTCQNYDL	
11	CTKTCQNYDLEC	
12	TKTCQNY	
13	TKTCQNYDLE	
14	TKTCQNYDLEC	
15	KTCQNYDLEC	
16	YDLEC	
17	MSMGCVSGCLCPPGMVRHENRCVA	
18	GCVSGCLCPPGMVRHENRC	
19	GCVSGCLCPPGMVRHENRCVA	
20	HQGKEYAPGET	E'
21	HQGKEYAPGETVKIGCN	
22	HQGKEYAPGETVKIGCNT	
23	STIGMAHY	VWD3
24	STIGMAHYLTF	
25	STIGMAHYLTFDGL	
26	STIGMAHYLTFDGLKYLFPGECQ	
27	STIGMAHYLTFDGLKYLFPGECQY	
28	IGMAHY	
29	IGMAHYLTF	
30	IGMAHYLTFDG	
31	IGMAHYLTFDGL	
32	IGMAHYLTFDGLKYLFPGE	
33	IGMAHYLTFDGLKYLFPGECQ	
34	MAHYLTF	
35	MAHYLTFDGL	
36	MAHYLTFDGLKYLFPGECQ	
37	AHYLTFDGLKYLFPGECQY	
38	LTFDGL	
39	LTFDGLKYLFPGECQ	
40	LTFDGLKYLFPGECQY	
41	FDGLKYLFPGECQ	
42	FDGLKYLFPGECQY	
43	DGLKYLFPGE	
44	DGLKYLFPGEC	

45	DGLKYLFPGECQ	
46	DGLKYLFPGECQY	
47	DGLKYLFPGECQYVL	
48	KYLFPGEC	
49	KYLFPGECQ	
50	KYLFPGECQY	
51	KYLFPGECQYVL	
52	YVLVQDYCGSNPGTF	
53	VLVQDYCGSNPGT	
54	VLVQDYCGSNPGTF	
55	VQDYCGSNPGTF	
56	YCGSNPGTF	
57	FRILVGNKGCSHPSVKCKKRVTIL	
58	RILVGNKGCSHPSVKCKKRVTIL	
59	VEGGEIE	
60	VEGGEIEL	
61	IELFDGEVNVKRPMKDETHF	
62	LFDGEVNVKRPMKDETHF	
63	FDGEVNVKRPMKDETHF	
64	EVNVKRPMKDETHF	
65	VNVKRPMKDETHF	
66	VKRPMKDETHF	
67	EVVESGRY	
68	IILLLGKALSV	
69	IILLLGKALSVVW	
70	IILLLGKALSVVWDRHLSIS	
71	IILLLGKALSVVWDRHLSISV	
72	LLGKALS	
73	LLGKALSV	
74	LLGKALSVVW	
75	LLGKALSVVWDRHLSI	
76	LLGKALSVVWDRHLSIS	
77	LLGKALSVVWDRHLSISV	
78	LGKALSV	
79	LGKALSVVW	
80	LGKALSVVWDRHLSI	
81	LGKALSVVWDRHLSIS	
82	LGKALSVVWDRHLSISV	
83	LGKALSVVWDRHLSISVV	
84	GKALSVVWDRHLSIS	
85	LSVVWDRHLSIS	
86	LSVVWDRHLSISV	
87	SVVWDRHLSISV	
88	VVWDRHLSIS	
89	VVWDRHLSISV	
90	VWDRHLSI	

91	VWDRHLSIS	
92	VWDRHLSISV	
93	DRHLSISV	
94	VVLKQTYQ	
95	VVLKQTYQE	
96	VVLKQTYQEKVCG	
97	VVLKQTYQEKVCGL	
98	VVLKQTYQEKVCGLCGNF	
99	VLKQTYQ	
100	VLKQTYQE	
101	VLKQTYQEKVCG	
102	VLKQTYQEKVCGL	
103	LKQTYQE	
104	LKQTYQEKVCGL	
105	KQTYQE	
106	KQTYQEKVCG	
107	KQTYQEKVCGL	
108	KQTYQEKVCGLCGNF	
109	KVCGLCGNF	
110	CGNFDGIQNNDL	
111	CGNFDGIQNNDLTSSNL	
112	DGIQNND	
113	DGIQNNDLTSSNL	
114	QVEEDPVDFGNS	
115	QVEEDPVDFGNSW	
116	PVDFGNS	
117	PVDFGNSW	
118	WKVSSQ	
119	WKVSSQC	
120	WKVSSQCA	
121	WKVSSQCAD	
122	WKVSSQCADT	
123	WKVSSQCADTRKVPLDSSPATCHN	
124	WKVSSQCADTRKVPLDSSPATCHNNIM	
125	WKVSSQCADTRKVPLDSSPATCHNNIMKQTMVDSSC	
126	CADTRKVPLDSSPATCHN	C8_3
127	CADTRKVPLDSSPATCHNNIM	
128	ADTRKVPLDSSPATCHN	
129	ADTRKVPLDSSPATCHNNIM	
130	DTRKVPLDSSPATCHN	
131	DTRKVPLDSSPATCHNNIM	
132	TRKVPLDSSPATCHN	
133	TRKVPLDSSPATCHNNI	
134	RKVPLDSSPATCHN	
135	RKVPLDSSPATCHNNIM	
136	KQTMVDSS	

137	RILTSDV	
138	DVFQDCNKLVDPEPYL	
139	FQDCNKLVDPEPYL	
140	FQDCNKLVDPEPYLDV	
141	YAHVCAQHGKVVT	
142	YAHVCAQHGKVVTW	
143	YAHVCAQHGKVVTWRTATL	
144	YAHVCAQHGKVVTWRTATLCPQSC	
145	EERNLRE	TIL3
146	EERNLRENGYESE	
147	RNLRENGYESE	
148	LRENGYESE	
149	WRYNSCAPAC	
150	WRYNSCAPACQ	
151	WRYNSCAPACQV	
152	RYNSCAPACQ	
153	QVTCQHPEPLAC	
154	VTCQHPEPLAC	
155	VTCQHPEPLACPVQ	
156	VTCQHPEPLACPVQCVEGCHAHCPPGKILDEL	
157	TCQHPEPLAC	
158	TCQHPEPLACPVQ	
159	PVQCVEGCHAHCPPGKILDEL	
160	PVQCVEGCHAHCPPGKILDELLQTCVDPEDCPVCE	
161	CVEGCHAHCPPGKILDEL	
162	CVEGCHAHCPPGKILDELL	
163	CVEGCHAHCPPGKILDELLQTCVDPEDCPVCE	
164	VEGCHAHCPPGKILDEL	
165	VEGCHAHCPPGKILDELLQTCVDPEDCPVCE	
166	GCHAHCPPGKILDELLQTCVDPEDCPVCE	
167	CVDPEDCPVCE	
168	EVAGRRFASGKKVTLNPSDPEHCQICHC	
169	VAGRRFASGKKVTLNPSDPEHC	E3
170	VAGRRFASGKKVTLNPSDPEHCQICHC	
171	VAGRRFASGKKVTLNPSDPEHCQICHCDV	
172	KVTLNPSDPEHCQICHC	
173	VTLNPSDPEHCQICHC	
174	PSDPEHCQICHC	
175	QICHC	
176	DVVNLTC	
177	DVVNLTCE	
178	ACQEPGGL	

Supplemental Table S1. Primary sequence and peptide numbers of the peptides identified using HDX-MS.